AJNR

Changes in Integrity of Normal-Appearing White Matter in Patients with Moyamoya Disease: A Diffusion Tensor Imaging Study

H. Jeong, J. Kim, H.S. Choi, E.S. Kim, D.-S. Kim, K.-W. Shim and S.-K. Lee

Changes in Integrity of Normal-Appearing White Matter in Patients with Moyamoya Disease: A Diffusion Tensor Imaging Study

H. Jeong
J. Kim
H.S. Choi
E.S. Kim
D.-S. Kim
K.-W. Shim
S.-K. Lee

BACKGROUND AND PURPOSE: DTI is widely used for the evaluation of white matter integrity in various neurologic diseases. The purpose of this study was to investigate changes in white matter integrity by using DTI in NAWM of patients with MMD and to evaluate the correlation between diffusion and perfusion characteristics through an interhemispheric comparison.

MATERIALS AND METHODS: We retrospectively reviewed 20 primary MMD patients with asymmetric disease stage and 20 age-matched healthy controls. FA_{CS} and ADC_{CS} values of bilateral centrum semiovale were measured by using region of interest analysis. Mean FA_{CS} and ADC_{CS} were compared between patient and control groups by unpaired t test. Interhemispheric differences in FA_{CS} and ADC_{CS} were assessed and compared between the $H\text{-}TTP_{delayed}$ and the $H\text{-}TTP_{shorter}$ by using paired t test. AIs also were assessed to verify interhemispheric differences.

RESULTS: The patient group showed a significantly lower mean FA_{CS} and a higher mean ADC_{CS} value than the control group. In the patient group, the $H\text{-}TTP_{delayed}$ had a significantly lower FA_{CS} and higher ADC_{CS} value than the $H\text{-}TTP_{shorter}$. Both AI_{FA} and AI_{ADC} were significantly higher in the patient compared with the control group.

CONCLUSIONS: DTI can describe subtle changes in white matter integrity in NAWM of patients with primary MMD that are not detected by conventional MR imaging. In addition, diffusion characteristics are well correlated with perfusion characteristics. We believe that DTI is a useful ancillary tool to evaluate patients with MMD.

ABBREVIATIONS: ADC_{CS} = apparent diffusion coefficient in centrum semiovale; AI = asymmetric index; FA_{CS} = fractional anisotropy in centrum semiovale; $H\text{-}TTP_{delayed}$ = hemisphere with more delayed time-to-peak; $H\text{-}TTP_{shorter}$ = contralateral hemisphere of $H\text{-}TTP_{delayed}$; MMD = Moyamoya disease; NAWM = normal-appearing white matter; PWI = perfusion-weighted MR imaging; rCBV = relative cerebral blood volume

MMD is a chronic steno-occlusive disease of the internal carotid arteries that mainly affects children. Various imaging techniques have been applied to evaluate the hemodynamic status, tissue integrity, and prognosis of MMD.[1-3]

The recent development of DTI has allowed visualization of fiber orientation and microstructural integrity in white matter and is considered to be a very useful tool for evaluating white matter in various central nervous system diseases.[4-7] DTI has been accepted as a tool with sufficient sensitivity to detect brain pathologies hidden in NAWM.[8-11] For example, DTI can reveal microstructural damage of NAWM in patients with chronic cerebral arterial occlusive disease.[11,12]

In patients with MMD, progressive vascular stenosis causes chronic cerebral hypoperfusion in the territory of the internal carotid arteries, but partial adaptation occurs through collateral blood flow from the posterior circulation, the ethmoidal vessel, and other basal vessels.[13] MMD with partially adapted chronic hypoperfusion follows a dynamic disease process. Patients with MMD may experience serial ischemic attacks, and some patients eventually experience cerebral infarct. We hypothesized that NAWM in MMD patients without cerebral infarct may be affected by chronic hypoperfusion, and DTI could reveal cumulative microstructural damage that is not visualized by conventional MR imaging.

Perfusion MR imaging has been found to be effective in the evaluation of cerebral hemodynamics in MMD.[3,14-16] TTP images are simple to use for the assessment of collateral status, development of neovascularization after encephaloduroarteriosyangiosis, and general perfusion status. In addition, the ischemic hemisphere usually shows an increased rCBV due to compensatory vasodilation and delayed TTP due to proximal vessel stenosis.[17] In MMD without infarction, an interhemispheric difference in TTP may be present due to different stages of proximal vessel stenosis. We hypothesized that the hemisphere with more delayed TTP ($H\text{-}TTP_{delayed}$) may be vulnerable to hypoperfusion, so NAWM in the $H\text{-}TTP_{delayed}$ may demonstrate a higher level of cumulative microstructural damage than NAWM in the contralateral hemisphere.

Thus, the purpose of this study was to investigate changes in white matter integrity by using DTI in NAWM of patients with MMD and to evaluate the correlation between diffusion and perfusion characteristics by an interhemispheric comparison.

Materials and Methods

Patients and Control Subjects

The institutional review board approved this retrospective study and waived the requirement for informed consent from patients or legal guardians. We retrospectively reviewed brain MR images and clinical data of 103 childhood MMD patients from August 2006 to August 2009 at the Severance Hospital of the Yonsei University Health System of Korea. Of these patients, 20 (15 girls and 5 boys; mean age, 9.55 years; range, 5–15 years) who satisfied the following criteria were included in the patient group: 1) patients who were diagnosed with primary childhood MMD on MR imaging and MRA according to the diagnostic criteria and guidelines for MMD proposed by the Research Committee on Spontaneous Occlusion of the Circle of Willis[18]; 2) patients who simultaneously underwent FLAIR imaging, MRA, PWI imaging, and DTI; 3) patients who had no clinical history of therapeutic intervention, such as pharmacotherapy (vasodilator or anticoagulant) or surgery (bypass or indirect revascularization procedure) before undergoing MR imaging; 4) patients who had no overt cerebral infarct on conventional MR imaging; and 5) patients who showed definitive asymmetric involvement upon visual analysis of MRA and TTP maps. Thirty-seven patients satisfied criteria 1–4, and 20 among them satisfied criteria 5 and were therefore included in the final patient group.

Because healthy childhood volunteers were not available due to the sedation procedure, "closest-to-normal" control diffusion data were obtained from 20 age-matched children (7 girls and 13 boys; mean age, 9.75 years; age range, 5–15 years) who had no vascular pathology on either radiologic or clinical evaluation. The control subjects had the following indications for MR imaging: central nervous system symptoms (headache, 12 patients; seizure, 2 patients) or psychiatric problems (schizophrenia, 2 patients; social phobia, 2 patients; adjustment disorder, 1 patient; conversion disorder, 1 patient). Conventional MR imaging and DTI were simultaneously performed on controls during the same period as for patient subjects.

Data Acquisition

All examinations were performed by 3T MR imaging (Achieva; Philips Medical Systems, Best, the Netherlands) by using an 8-channel sensitivity-encoding head coil. DTI, PWI, MRA, FLAIR, T2-weighted, and gradient-echo T2*-weighted images were obtained in patients with MMD. T1-weighted, T2-weighted, and postcontrast T1-weighted images and DTI were obtained in the control group.

DTI was performed by using single-shot spin-echo-EPI. The axial images were obtained parallel to the anterior/posterior commissure line. The parameters for DTI were as follows: TR/TE/flip angle = 6000 ms/100 ms/90°, FOV = 22 cm, acquisition matrix = 128 × 128, section thickness/intersection gap = 5 mm/2 mm, and NEX = 4. Diffusion sensitizing gradient encoding was applied in 6 directions (x, y, z, xy, yz, and zx) with b at 1000 seconds/mm^2, and 1 image was acquired without by using a diffusion gradient (with b at 0). Isotropic ADC, trace, and FA maps were immediately generated on the console by research software (Packman Tools; Philips Medical Systems). The 6 elements of the diffusion tensor were estimated in each voxel assuming a mono-exponential relationship between signal intensity and the b-matrix. Using multivariate regression, the eigenvectors and eigenvalues of the diffusion tensor were determined. To minimize the eddy current–related artifact, we implemented zero and first-order eddy current compensations into the MR imaging system and monitored and calibrated the eddy current level.
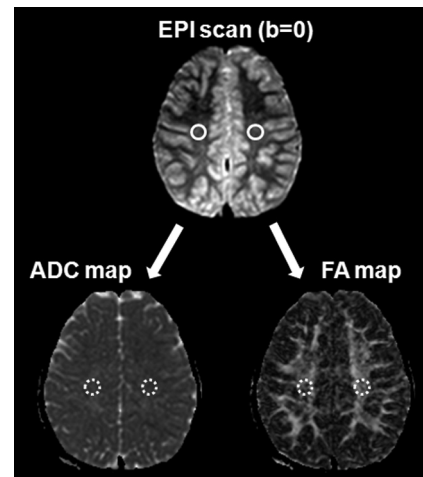

Fig 1. ROI method for ADC$_{CS}$ and FA$_{CS}$ measurement. Round ROIs (60 mm^3) were drawn on the EPI scan of the $b = 0$ step at the level of the centrum semiovale, followed by automatic overlaying onto the coregistered FA and ADC images.

PWI was carried out by using multishot gradient-echo principles of echo shifting with a train of observations technique by using the following parameters: TR/TE/flip angle = 2000/60/90°, matrix = 128 × 128, FOV = 24 cm, and section thickness/intersection gap = 5 mm/2 mm. All 60 phase images were obtained before, during, and after the administration of contrast agent (0.1 mmol of gadopentetate dimeglumine [Magnevist; Schering, Berlin, Germany] per kilogram of body weight at a rate of 2 mL/s) through an MR imaging–compatible power injector (Spectris; Medrad, Indianola, Pennsylvania) in those patients older than 5 years or by manual injection in those patients 5 years and younger. This injection was followed by a 15-mL bolus of saline administered at the same injection rate. Perfusion maps of TTP and CBV were generated after eliminating the effect of contrast agent recirculation by γ-variate curve fitting.[19,20]

MRA was obtained with the 3D time-of-flight technique with a 3D spoiled gradient recalled-echo sequence by using the following parameters: TR/TE/flip angle = 24/3.45/20°, matrix = 512 × 208, FOV = 20 cm, section thickness = 0.8 mm, and effective voxel size = 0.39 × 0.96 × 0.8 mm.

Conventional T1-weighted (TR/TE/flip angle, 2000 ms/10 ms/90°), FLAIR (TR/TE/TI, 11,000 ms/125 ms/2800 ms), T2-weighted (TR/TE, 3000 ms/80 ms), and gradient-echo T2*-weighted (TR/TE/flip angle, 576 ms/15 ms/18°) images were obtained by using the respective parameters.

Data Analysis

In each MMD patient, the H-TTP$_{delayed}$ and the greater degree of proximal vessel stenosis was determined by the consensus of 2 radiologists (H.J. with 3 years of experience in MR imaging interpretation and S.-K.L. with 13 years of experience) by visual analysis of the TTP map and by using the MRA scoring system proposed by Houkin et al.[21] The rCBV patterns in the areas with more delayed TTP also were visually evaluated.

ADC and FA values were measured in the bilateral centrum semiovale of both patient and control groups. The software program NeuRoi (Dr C. Tench, Department of Clinical Neurology, University of Nottingham, United Kingdom), was used for semiautomatic measurement. This program is available at www.nottingham.ac.uk/scs/divisions/clinicalneurology/index.aspx. The ROIs in the centrum

Table 1: Clinical information and findings for TTP status, degree of supraclinoid ICA or MCA stenosis, and rCBV pattern

No.	Sex	Age (yr)	Clinical Symptom	H-TTP$_{delayed}$	MRA Score[a] Rt.	MRA Score[a] Lt.	rCBV in H-TTP$_{delayed}$
1	F	5	TIA (Lt. HP)	Rt.	2	1	Increased
2	M	6	TIA (Rt. HP)	Lt.	3	4	Increased
3	F	6	TIA (Rt. HP)	Lt.	1	4	Increased
4	F	6	Headache	Rt.	4	3	Increased
5	F	6	TIA (Rt. HP)	Rt.	3	1	Increased
6	F	7	TIA (Rt. HP)	Lt.	3	4	Increased
7	F	7	Seizure	Lt.	1	2	Increased
8	F	8	TIA (Rt. HP)	Lt.	4	5	Increased
9	F	8	Headache	Lt.	2	3	Increased
10	F	8	Family history	Lt.	3	4	Increased
11	M	10	TIA (Lt. HP)	Lt.	4	5	Increased
12	F	10	TIA (Rt. HP)	Lt.	2	3	Increased
13	M	11	TIA (Rt. HP)	Lt.	2	3	Increased
14	M	12	Headache	Lt.	1	2	Increased
15	F	12	TIA (Lt. HP)	Rt.	5	1	Increased
16	M	13	Hypogonadism	Lt.	1	3	Increased
17	F	13	TIA (Lt. HP)	Lt.	2	3	Increased
18	F	13	TIA (Rt. HP)	Lt.	3	5	Increased
19	F	15	TIA (Rt. HP)	Lt.	3	5	Increased
20	F	15	TIA (Lt. HP)	Rt.	4	2	Increased

Note:—HP indicates hemisphere
[a] MRA score is presented as the sum of anterior cerebral artery, MCA, posterior cerebral artery, and distal ICA using the MRA scoring system proposed by Houkin et al.[21]

Table 2: Measured diffusion characteristics in patient and control groups

	Patient Group H-TTP$_{delayed}$ FA$_{CS}$	Patient Group H-TTP$_{delayed}$ ADC$_{CS}$	Patient Group H-TTP$_{shorter}$ FA$_{CS}$	Patient Group H-TTP$_{shorter}$ ADC$_{CS}$	Control Group H-TTP$_{delayed}$ FA$_{CS}$	Control Group H-TTP$_{delayed}$ ADC$_{CS}$	Control Group H-TTP$_{shorter}$ FA$_{CS}$	Control Group H-TTP$_{shorter}$ ADC$_{CS}$
Patient								
1	438	837.5	486	831.7	420.7	797.6	415.7	788.2
2	445.4	783.8	408	814.7	431.3	951.5	426	829
3	438	836.3	487	779.8	464.2	781.1	454.7	807.9
4	505.6	754.4	445.1	795.5	513.3	749.4	475.6	769.3
5	458.4	934.1	528.2	814.3	454.5	830.9	448.2	804.5
6	388	864	399.9	862.6	486.4	738.8	478.9	743.4
7	406.4	860.8	391.3	863.4	506.4	719.2	484.3	709.1
8	463.8	767	425.4	765.9	472.2	754.7	476	730.2
9	464.2	759.1	425.9	792.9	468.5	773.3	488.4	765.3
10	502.6	748.2	471.2	741.6	501.2	728.8	505.1	717.4
11	521.9	723.9	490.2	707.2	556.2	703.1	512.3	702
12	554.5	774.6	517.6	801.2	522.9	785.6	543.9	765.6
13	492.2	802.5	433	806.9	550.4	722.7	524.9	687.4
14	541.2	713.3	511.7	756.2	504.1	737.1	495.1	705.3
15	439.3	801.3	496.6	741.6	555	728.2	526.8	716.6
16	458	759.1	425	733.3	518.8	846.1	576.5	799.4
17	516.4	742.4	485.9	802.4	462.2	750.8	487.5	686.2
18	484.8	707	465.3	756.8	452.7	830.1	469.1	775.4
19	427.4	794.4	417.4	782.9	584.3	685.1	583.1	666.1
20	462.4	747.4	418.8	798.2	555.3	869.6	589.7	820.3

Note:—FA values ($\times 10^{-3}$); ADC values (mm^2/s).

semiovale were drawn manually in a 60-mm^3 round shape. To avoid contamination from adjacent CSF and gray matter, the ROIs were drawn on the EPI scan of the $b = 0$ step (T2-weighted, but not diffusion-weighted) at the level of the centrum semiovale, and then automatically overlaid onto the coregistered FA and ADC images (Fig 1). To ensure consistency and consensus, 1 investigator (H.J.) drew the ROIs and 1 board-certified neuroradiologist (S.-K.L.) subsequently confirmed them.

Statistical Analysis
We compared the FA and ADC values between the patient and control groups by using the independent samples t test. We then

Table 3: Comparison of diffusion characteristics between patient and control groups

	Patient Group	Control Group	P
Mean FA$_{CS}$ ($\times 10^{-3}$)	463.45 ± 43.14		.0008[a]
Mean ADC$_{CS}$ (mm^2/s)	786.50 ± 49.20	751.55 ± 56.91	.0043[a]

Note:—Values are presented as the mean ± SD.
[a] Significant difference between groups ($P < .05$).

compared the diffusion characteristics of H-TTP$_{delayed}$ and the H-TTP$_{shorter}$ in the patient group by using the paired samples t test.

Because diffusion characteristics in the normal brain are somewhat asymmetrical,[22] AIs also were used to verify the significance of

Table 4: Interhemispheric comparison of diffusion characteristics

	Patient Group		Control Group	
	H-TTP$_{delayed}$	H-TTP$_{shorter}$	Rt.	Lt.
In each group				
Mean FA$_{CS}$ ($\times 10^{-3}$)	445.77 ± 35.09	481.13 ± 43.93	499.03 ± 45.85	498.09 ± 48.46
P		<.0001[a]	.8682	
Mean ADC$_{CS}$ (mm²/s)	800.12 ± 51.52	772.89 ± 43.86	753.68 ± 64.75	749.43 ± 49.47
P		.0022[a]	.5709	
Asymmetric index				
AI$_{FA}$	0.075 ± 0.04		0.0023 ± 0.04	
P		<.0001[a]		
AI$_{ADC}$	0.034 ± 0.04		0.004 ± 0.04	
P		.0294[a]		

Note:—Values are presented as the mean ± SD.
[a] Significant difference between groups (P <.05).

the difference between H-TTP$_{delayed}$ and H-TTP$_{shorter}$. The mathematic equations providing AI for FA values in the centrum semiovale were as follows:

$$AI \text{ in patient group} = (FA\text{-}H\text{-}TTP_{shorter} - FA\text{-}H\text{-}TTP_{delayed})/$$
$$0.5 \times (FA\text{-}H\text{-}TTP_{shorter} + FA\text{-}H\text{-}TTP_{delayed})$$

$$AI \text{ in control group} = (FA_{Rt} - FA_{Lt})/(0.5 \times (FA_{Rt} + FA_{Lt}))$$

where $FA\text{-}H\text{-}TTP_{shorter}$ is the FA value in the H-TTP$_{shorter}$ (FA-H-TTP$_{shorter}$), $FA\text{-}H\text{-}TTP_{delayed}$ is the FA value in the H-TTP$_{delayed}$ (FA-H-TTP$_{delayed}$), FA_{Rt} is the FA value in the right hemisphere, and FA_{Lt} is the FA value in the left hemisphere.

The same pattern of mathematic equations also was applied to the ADC values. The independent samples t test was used to compare AI between patient and control groups.

A probability of <5% was considered statistically significant. All statistical analyses were performed by using MedCalc 7.4.0.0 software (MedCalc, Mariakerke, Belgium).

Results

The clinical information and findings pertaining to the hemisphere with TTP$_{delayed}$ and greater degree of proximal vessel stenosis among the bilateral hemispheres, and the rCBV pattern are summarized in Table 1. Fourteen of the 20 MMD patients presented with recurrent TIA. In patients with recurrent TIA, H-TTP$_{delayed}$ was highly concordant with the symptomatic hemisphere (95%). The detailed FA and ADC values in each group are summarized in Table 2.

The patient group showed a significantly lower mean FA$_{CS}$ value and a higher mean ADC$_{CS}$ value compared with the control group (Table 3). The results of the interhemispheric comparison are summarized in Table 4. In the patient group, H-TTP$_{delayed}$ showed a significantly lower FA$_{CS}$ value and a higher ADC$_{CS}$ value compared with H-TTP$_{shorter}$ (Fig 2). There were no significant differences in the mean FA and ADC values between the right and left centrum semiovales in the control group. Both AI$_{FA}$ and AI$_{ADC}$ were significantly higher in the patient group compared with the control group.

Discussion

We demonstrated that DTI could detect the cumulative microstructural damage that was not detected on conventional MR imaging in the NAWM with chronic hypoperfusion in primary childhood MMD without overt infarction. In ad-

dition, we revealed that the NAWM of the hemisphere with more delayed perfusion in each MMD patient had more microstructural damage.

The 2 most commonly determined diffusion properties are the FA, reflecting the degree to which the diffusion tensor deviates from isotropy, and the ADC, reflecting the orientation-averaged apparent diffusivity.[7] The FA value may be low when white matter integrity is disrupted. Several studies revealed that the FA value is an indicator of tissue damage in the white matter despite the absence of definite abnormalities on conventional T2 or FLAIR images.[11,12,23] The net diffusion of water molecules measured in a particular tissue is referred to as ADC.[5] In chronic hypoperfusion, ischemic injury to white matter is associated with axonal destruction and glial proliferation.[24] These microstructural changes are associated with an increase in the ADC, probably reflecting increased water diffusivity due to axonal loss.[25] However, ADC changes are not confined to ischemic lesions and may occur in NAWM.[11,26-28] Thus, we investigated changes in integrity of NAWM with MMD, by using measurements of both FA and ADC.

Our results showed that NAWM of MMD patients without infarction had a significantly lower mean FA$_{CS}$ value and a higher mean ADC$_{CS}$ value compared with controls. There have been a few previous DTI studies for MMD. Using whole brain histogram analysis, Mori et al[29] revealed that MMD with infarction had significantly lower FA and mean diffusivity than controls. Moreover, they reported that MMD without infarction showed the same tendency, though the differences were not statistically significant. The discrepancy in statistical significance between our study and that of Mori et al[29] can be explained by differences in data analysis. The whole brain histogram is an accurate and robust method for overall measurements, but it cannot reveal results in a specific site. We therefore assume that in our study the localized regional analysis for centrum semiovale revealed significant differences in diffusion characteristics, suggesting microstructural damage in the NAWM of patients with MMD without infarction. Recently, Conklin et al[30] revealed that regions of steal phenomenon are spatially correlated with elevated ADC in NAWM of patients with MMD, suggesting that even if there is no overt infarction in MMD, microstructural damage of NAWM can develop from low-grade ischemia. Our finding of increased ADC in NAWM of patients with MMD without infarction is
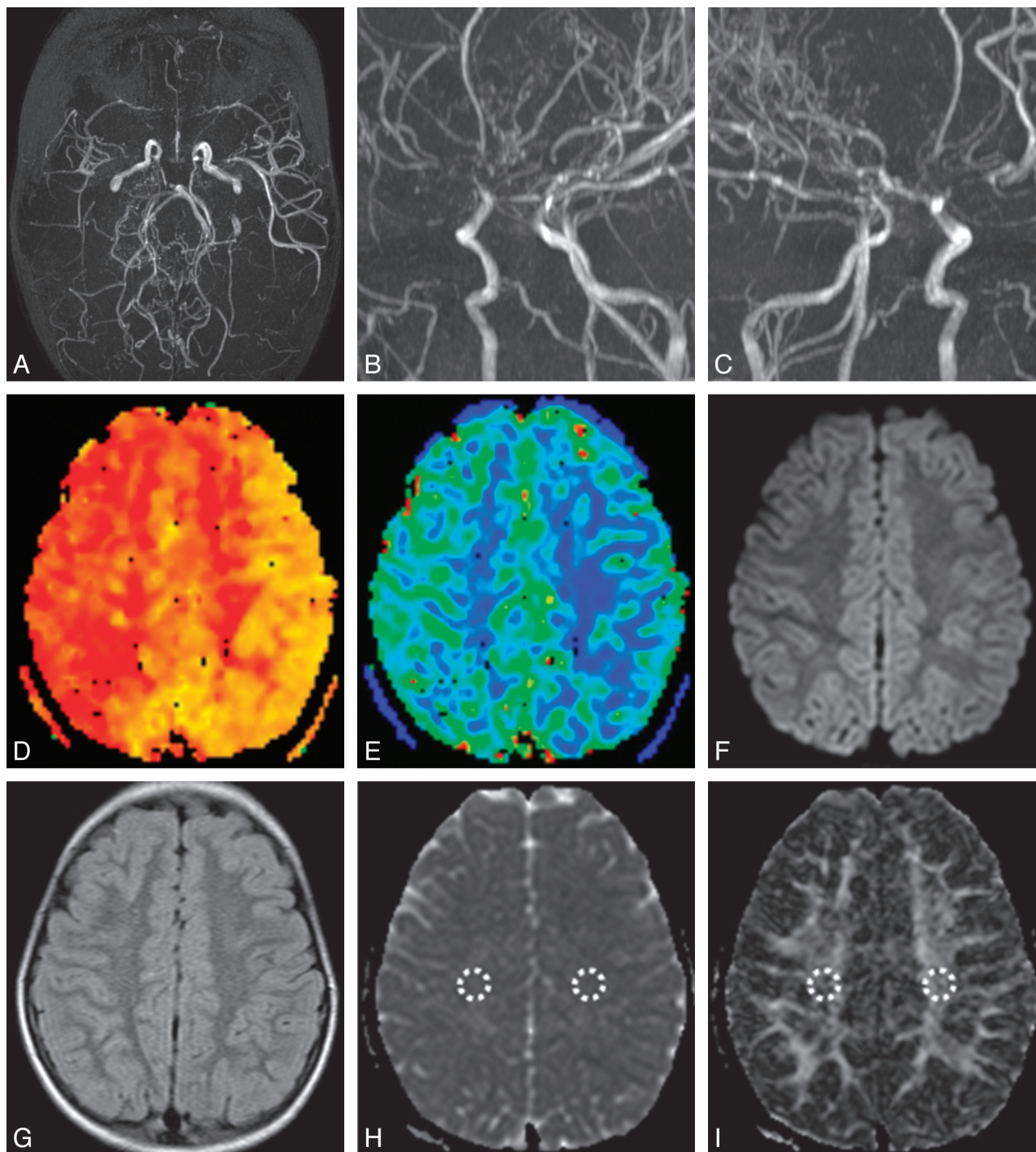
Fig 2. Primary MMD in a 6-year-old girl. *A–C*, MRA images showed asymmetric MRA cores and stages between both hemispheres (Rt., stage III; Lt., stage II). TTP (*D*) and CBV (*E*) maps demonstrated asymmetric hemodynamic status, in which the Rt. hemisphere showed more delayed TTP and increased CBV. Diffusion-weighted image ($b = 1000$; *F*) and a FLAIR image (*G*) did not show any abnormalities. *H*, ADC map, right side ADC_{CS} (836.3 mm^2/s) was higher than left side ADC_{CS} (779.8 mm^2/s). *I*, FA map, right side FA_{CS} (0.438 $\times$ 10^{-3}) was lower than left side FA_{CS} (0.487 $\times$ 10^{-3}).

consistent with the findings of Conklin et al.[30] We found a significantly lower mean FA_{CS} value and a higher mean ADC_{CS} value in patients with MMD, probably reflecting cumulative white matter damage from chronic hypoperfusion and recurrent ischemic attacks.

Next, we analyzed the interhemispheric DTI difference in patients with MMD who showed asymmetric TTP status. MMD was defined as bilateral disease, but MMD is known to have a rather asymmetric perfusion appearance, especially in children. MMD also can show a somewhat asymmetric disease status in chronic progressive disease. This asymmetric disease status in MMD can be detected on MRA and PWI. In MMD, the hypoperfused hemisphere usually shows increased rCBV due to compensatory vasodilation, and delayed TTP represents proximal occlusion or stenosis and collateral flow. Our results showed that the hemisphere with a more delayed TTP

and a higher MRA score had a significantly lower FA_{CS} value and a higher ADC_{CS} value than the more perfused contralateral hemisphere. This result may reflect that NAWM of $H\text{-}TTP_{delayed}$ is more vulnerable to hypoperfusion than the more perfused contralateral hemisphere and that NAWM in $H\text{-}TTP_{delayed}$ may demonstrate more cumulative microstructural damage than NAWM in the contralateral hemisphere.

We note that our study has some limitations. First, the retrospective data analysis resulted in a reduced number of enrolled patients with a high degree of homogeneity in terms of disease and age. Second, for ethical reasons, ideal healthy control subjects were not recruited and structurally normal children's brains were used for comparison. However, we speculate that our results would not have been too different if this study had been performed with ideal controls. Third, DTI in this study was performed with only 6 different diffusion gradients. It has been reported that at least 20 diffusion gradients are necessary for a robust estimation of diffusion characteristics.[31] The small number of diffusion gradients in our study could thus be a limitation. Fourth, the lack of absolute quantification in perfusion MR imaging is another limitation. Thus, future investigation by using quantitative analysis of PWI and DTI with at least 20 diffusion gradients is needed.

Conclusions

DTI can detect subtle changes in white matter integrity in chronic hypoperfused brains of patients with primary childhood MMD that are not detected by conventional MR imaging. In addition, diffusion and perfusion characteristics are well correlated. Our findings suggest that DTI can be used as an ancillary tool to evaluate disease severity of patients with primary childhood MMD.

References

1. Suzuki J, Takaku A. **Cerebrovascular "Moyamoya" disease. Disease showing abnormal net-like vessels in base of brain.** *Arch Neurol* 1969;20:288–99
2. Yamada I, Himeno Y, Nagaoka T, et al. **Moyamoya disease: evaluation with diffusion-weighted and perfusion echo-planar MR imaging.** *Radiology* 1999;212:340–47
3. Calamante F, Ganesan V, Kirkham FJ, et al. **MR perfusion imaging in Moyamoya syndrome: potential implications for clinical evaluation of occlusive cerebrovascular disease.** *Stroke* 2001;32:2810–16
4. Le Bihan D. **Diffusion, perfusion and functional magnetic resonance imaging.** *J Mal Vasc* 1995;20:203–14
5. Le Bihan D, Breton E, Lallemand D, et al. **MR imaging of intravoxel incoherent motions: application to diffusion and perfusion in neurologic disorders.** *Radiology* 1986;161:401–07
6. Chenevert TL, Brunberg JA, Pipe JG. **Anisotropic diffusion in human white matter: demonstration with MR techniques in vivo.** *Radiology* 1990;177:401–05
7. Basser PJ, Pierpaoli C. **Microstructural and physiological features of tissues elucidated by quantitative-diffusion-tensor MRI.** *J Magn Reson B* 1996;111:209–19
8. Buchsbaum MS, Tang CY, Peled S, et al. **MRI white matter diffusion anisotropy and PET metabolic rate in schizophrenia.** *Neuroreport* 1998;9:425–30
9. Werring DJ, Clark CA, Barker GJ, et al. **Diffusion tensor imaging of lesions and normal-appearing white matter in multiple sclerosis.** *Neurology* 1999;52:1626–32
10. Chabriat H, Pappata S, Poupon C, et al. **Clinical severity in CADASIL related to ultrastructural damage in white matter: in vivo study with diffusion tensor MRI.** *Stroke* 1999;30:2637–43
11. O'Sullivan M, Summers PE, Jones DK, et al. **Normal-appearing white matter in ischemic leukoaraiosis: a diffusion tensor MRI study.** *Neurology* 2001;57:2307–10
12. Shiraishi A, Hasegawa Y, Okada S, et al. **Highly diffusion-sensitized tensor imaging of unilateral cerebral arterial occlusive disease.** *AJNR Am J Neuroradiol* 2005;26:1498–504
13. Miyamoto S, Kikuchi H, Karasawa J, et al. **Study of the posterior circulation in Moyamoya disease. Clinical and neuroradiological evaluation.** *J Neurosurg* 1984;61:1032–37
14. Kim SK, Wang KC, Oh CW, et al. **Evaluation of cerebral hemodynamics with perfusion MRI in childhood Moyamoya disease.** *Pediatr Neurosurg* 2003;38:68–75
15. Tanaka Y, Nariai T, Nagaoka T, et al. **Quantitative evaluation of cerebral hemodynamics in patients with Moyamoya disease by dynamic susceptibility contrast magnetic resonance imaging—comparison with positron emission tomography.** *J Cereb Blood Flow Metab* 2006;26:291–300
16. Yun TJ, Cheon JE, Na DG, et al. **Childhood Moyamoya disease: quantitative evaluation of perfusion MR imaging—correlation with clinical outcome after revascularization surgery.** *Radiology* 2009;251:216–23
17. Lee SK, Kim DI, Jeong EK, et al. **Postoperative evaluation of Moyamoya disease with perfusion-weighted MR imaging: initial experience.** *AJNR Am J Neuroradiol* 2003;24:741–47
18. Fukui M. **Guidelines for the diagnosis and treatment of spontaneous occlusion of the circle of Willis ('Moyamoya' disease). Research Committee on Spontaneous Occlusion of the Circle of Willis (Moyamoya Disease) of the Ministry of Health and Welfare, Japan.** *Clin Neurol Neurosurg* 1997;99 Suppl 2:S238–40
19. Ostergaard L, Weisskoff RM, Chesler DA, et al. **High resolution measurement of cerebral blood flow using intravascular tracer bolus passages. Part I: mathematical approach and statistical analysis.** *Magn Reson Med* 1996;36:715–25
20. Ostergaard L, Sorensen AG, Kwong KK, et al. **High resolution measurement of cerebral blood flow using intravascular tracer bolus passages. Part II: experimental comparison and preliminary results.** *Magn Reson Med* 1996;36:726–36
21. Houkin K, Nakayama N, Kuroda S, et al. **Novel magnetic resonance angiography stage grading for Moyamoya disease.** *Cerebrovasc Dis* 2005;20:347–54
22. Cao Y, Whalen S, Huang J, et al. **Asymmetry of subinsular anisotropy by in vivo diffusion tensor imaging.** *Hum Brain Mapp* 2003;20:82–90
23. Guo AC, MacFall JR, Provenzale JM. **Multiple sclerosis: diffusion tensor MR imaging for evaluation of normal-appearing white matter.** *Radiology* 2002;222:729–36
24. Pantoni L, Garcia JH. **Pathogenesis of leukoaraiosis: a review.** *Stroke* 1997;28:652–59
25. Helenius J, Soinne L, Salonen O, et al. **Leukoaraiosis, ischemic stroke, and normal white matter on diffusion-weighted MRI.** *Stroke* 2002;33:45–50
26. Soinne L, Helenius J, Saimanen E, et al. **Brain diffusion changes in carotid occlusive disease treated with endarterectomy.** *Neurology* 2003;61:1061–65
27. O'Sullivan M, Morris RG, Huckstep B, et al. **Diffusion tensor MRI correlates with executive dysfunction in patients with ischaemic leukoaraiosis.** *J Neurol Neurosurg Psychiatry* 2004;75:441–47
28. Engelter ST, Provenzale JM, Petrella JR, et al. **The effect of aging on the apparent diffusion coefficient of normal-appearing white matter.** *AJR Am J Roentgenol* 2000;175:425–30
29. Mori N, Miki Y, Fushimi Y, et al. **Cerebral infarction associated with Moyamoya disease: histogram-based quantitative analysis of diffusion tensor imaging—a preliminary study.** *Magn Reson Imaging* 2008;26:835–40
30. Conklin J, Fierstra J, Crawley AP, et al. **Impaired cerebrovascular reactivity with steal phenomenon is associated with increased diffusion in white matter of patients with Moyamoya disease.** *Stroke* 2010;41:1610–16
31. Jones DK. **The effect of gradient sampling schemes on measures derived from diffusion tensor MRI: a Monte Carlo study.** *Magn Reson Med* 2004;51:807–15